Dissociation and Vibrational Relaxation of XeF by Various Collision Partners

J. F. BOTT, R. F. HEIDNER, J. S. HOLLOWAY
J. B. KOFFEND, and M. A. KWOK
Aerophysics Laboratory
Laboratory Operations
The Aerospace Corporation
El Segundo, CA 90245

15 July 1989

Prepared for

SPACE SYSTEMS DIVISION
AIR FORCE SYSTEMS COMMAND
Los Angeles Air Force Base
P.O. Box 92960
Los Angeles, CA 90009-2960

This report was submitted by The Aerospace Corporation, El Segundo, CA 90245, under Contract No. F04701-85-C-0086-P00019 with the Space Systems Division, P.O. Box 92960, Los Angeles, CA 90009-2960. It was reviewed and approved for The Aerospace Corporation by W. P. Thompson, Director, Aerophysics Laboratory. Lt Scott W. Levinson was the project officer for the Mission-Oriented Investigation and Experimentation (MOIE) Program.

This report has been reviewed by the Public Affairs Office (PAS) and is releasable to the National Technical Information Service (NTIS). At NTIS, it will be available to the general public, including foreign nationals.

This technical report has been reviewed and is approved for publication. Publication of this report does not constitute Air Force approval of the report's findings or conclusions. It is published only for the exchange and stimulation of ideas.

SCOTT W. LEVINSON, LT, USAF
MOIE Project Monitor
SSD/CNID

JAMES A. BERES, LT COL, USAF
DIRECTOR, AFSTC/WCO OL-AB

UNCLASSIFIED

SECURITY CLASSIFICATION OF THIS PAGE

REPORT DOCUMENTATION PAGE

1a. REPORT SECURITY CLASSIFICATION Unclassified	1b. RESTRICTIVE MARKINGS
2a. SECURITY CLASSIFICATION AUTHORITY	3. DISTRIBUTION/AVAILABILITY OF REPORT Approved for public release; distribution unlimited.
2b. DECLASSIFICATION/DOWNGRADING SCHEDULE	
4. PERFORMING ORGANIZATION REPORT NUMBER(S) TR-0088(3930-04)-2	5. MONITORING ORGANIZATION REPORT NUMBER(S) SD-TR-89-39
6a. NAME OF PERFORMING ORGANIZATION The Aerospace Corporation Laboratory Operations 6b. OFFICE SYMBOL (If applicable)	7a. NAME OF MONITORING ORGANIZATION Space Systems Division
6c. ADDRESS (City, State, and ZIP Code) El Segundo, CA 90245	7b. ADDRESS (City, State, and ZIP Code) Los Angeles Air Force Base Los Angeles, CA 90009-2960
8a. NAME OF FUNDING/SPONSORING ORGANIZATION 8b. OFFICE SYMBOL (If applicable)	9. PROCUREMENT INSTRUMENT IDENTIFICATION NUMBER F04701-85-C-0086-P00019
8c. ADDRESS (City, State, and ZIP Code)	10. SOURCE OF FUNDING NUMBERS PROGRAM ELEMENT NO. / PROJECT NO. / TASK NO. / WORK UNIT ACCESSION NO.

11. TITLE (Include Security Classification)
Dissociation and Vibrational Relaxation of XeF by Various Collison Partners

12. PERSONAL AUTHOR(S)
Bott, Jerry F., Heidner, Raymond F., Holloway, John S., Koffend, John B., and Kwok, Munson A.

13a. TYPE OF REPORT	13b. TIME COVERED	14. DATE OF REPORT (Year, Month, Day)	15. PAGE COUNT
	FROM _____ TO _____	15 July 1989	23

16. SUPPLEMENTARY NOTATION-

17. COSATI CODES			18. SUBJECT TERMS (Continue on reverse if necessary and identify by block number)
FIELD	GROUP	SUB-GROUP	Chemical Kinetics; Vibrational Relaxation; Excimer Laser; Xenon Fluoride

19. ABSTRACT (Continue on reverse if necessary and identify by block number)

The removal rates of the lower levels of XeF strongly affect the overall efficiency of the XeF excimer laser operating on the B → X transitions. We have deduced the removal rates of XeF(X,v = 3) in krypton, xenon, nitrogen, and carbon dioxide and the removal rates of XeF(X,v = 0) in sulfur hexafluoride by monitoring the populations of vibrational levels formed by the photolysis of XeF_2. The time history of the selected vibrational population is monitored with a continuous-wave (cw) tunable dye laser tuned to an absorption feature of the selected vibrational/rotational level. The studies show a rapid vibrational relaxation followed by a common decay rate of the coupled vibrational levels. The rare gases were found to remove XeF(X) with rate coefficients that differed from one another by less than a factor of 1.6. Larger removal rate coefficients were measured for molecular collision partners, with XeF_2 having the largest rate coefficient. Rate coefficients were also determined for the concerted vibrational relaxation of v = 3 although the values do not represent state-to-

20. DISTRIBUTION/AVAILABILITY OF ABSTRACT	21. ABSTRACT SECURITY CLASSIFICATION
☐ UNCLASSIFIED/UNLIMITED ☒ SAME AS RPT. ☐ DTIC USERS	Unclassified
22a. NAME OF RESPONSIBLE INDIVIDUAL	22b. TELEPHONE (Include Area Code) / 22c. OFFICE SYMBOL

DD FORM 1473, 84 MAR 83 APR edition may be used until exhausted. All other editions are obsolete

SECURITY CLASSIFICATION OF THIS PAGE
UNCLASSIFIED

19. ABSTRACT (Continued)

state rate coefficients. Fast vibrational relaxation is required to empty the lower levels of the laser transitions so that vibrational "bottlenecking" does not terminate laser action prematurely.

CONTENTS

FIGURES

TABLES

I. INTRODUCTION

The performance of E-beam-pumped, high-pressure XeF lasers depends directly on the kinetic processes that produce and remove the vibronic levels of the upper electronic state, $B^2\Sigma^+$ (and also the coupled $C^2\pi^+$ state), and of the lower state, $X^2\Sigma^+,v''$. In particular, laser performance depends on the removal of the lower levels by vibrational redistribution or by dissociation of the weakly bound XeF(X).[1] Rapid dissociation of the ground state prevents the population of the lower levels of the laser transitions from building up and shutting off the laser action before a significant fraction of the available excitation energy is extracted. A knowledge of the values of the rate coefficients for the dissociation and vibrational relaxation of XeF(X) is required for modeling the performance of the XeF laser.

It is known[1,2] that the efficiency of the XeF B → X laser improves with temperature, at least up to about 425 K. One explanation for this increased efficiency is that the rates of vibrational relaxation and dissociation of the ground state increase with temperature faster than the rates of processes that remove the upper state or otherwise lower the gain of the laser. If an inert gas could be added to the laser mixture to remove rapidly the lower levels of the laser transitions without significantly deactivating the upper levels, the efficiency of the laser could be improved.

In previous studies, Fulghum et al.[3,4] and Bott et al.[5] have studied the removal and redistribution of XeF(X) by helium, neon, argon, and XeF_2. They found the removal rates to be similar for helium, neon, and argon but much faster for XeF_2. We have extended these studies to additional collision partners including krypton, xenon, carbon dioxide, nitrogen, and sulfur hexafluoride to determine if such collision partners might have removal rates as fast as that for XeF_2.

II. EXPERIMENTAL METHOD AND RESULTS

A convenient method of obtaining ground state XeF is the ultraviolet (UV) photolysis of XeF_2 with a 15-nsec ArF excimer laser pulse at 193 nm. The photolysis can produce XeF(X,v) directly or can produce electronically excited XeF(B), which decays with a 14-nsec lifetime[6] to the ground electronic state, XeF(X,v). Selected vibrational levels of the ground state are monitored with a frequency-doubled continuous wave (cw) ring dye laser tuned to absorption features near 350 nm. A schematic of the apparatus is shown in Fig. 1. The tunable dye laser beam passes through the cell containing the photolytically produced XeF(X) and is monitored with a photomultiplier whose signal is recorded with a transient digitizer and then averaged at the laser repetition rate of 5 Hz. The absorption of this dye laser beam depends directly on the concentration of the selected vibrational level of XeF. Therefore, the removal rate of that level by dissociation and vibrational relaxation can be determined from the time behavior of the transmitted signal. The details of the data collection and analysis have been previously described in Ref. 5.

An absorption feature in the 3 ← 0 band at a nominal wavelength of 353.323 nm (vacuum) was used for measurements of the removal rates of XeF(X,v = 3). The wavelength before doubling was measured with a Burleigh wavemeter Model WA-20 with an accuracy of 0.001 nm. This translates to an accuracy of 0.0005 nm near 350 nm for the doubled dye laser. The absorption profiles observed for v = 3 showed a fast, instrument-limited rise time followed by a double-exponential decay. An example of the measured absorption profiles is shown in Fig. 2 for XeF(X,v = 3) in N_2 at a total pressure of 7.4 Torr. The solid curve drawn through the measured profile is the least squares fit of an expression containing two exponentially decaying terms. The fit of such expressions to the measured profiles enabled us to extract the two decay rates. The first exponential decay rate can be attributed to vibrational relaxation processes that drive the population of v = 3 into equilibrium with the other vibrational populations. At long times, the several vibrational levels, coupled together by the fast vibration-to-translation

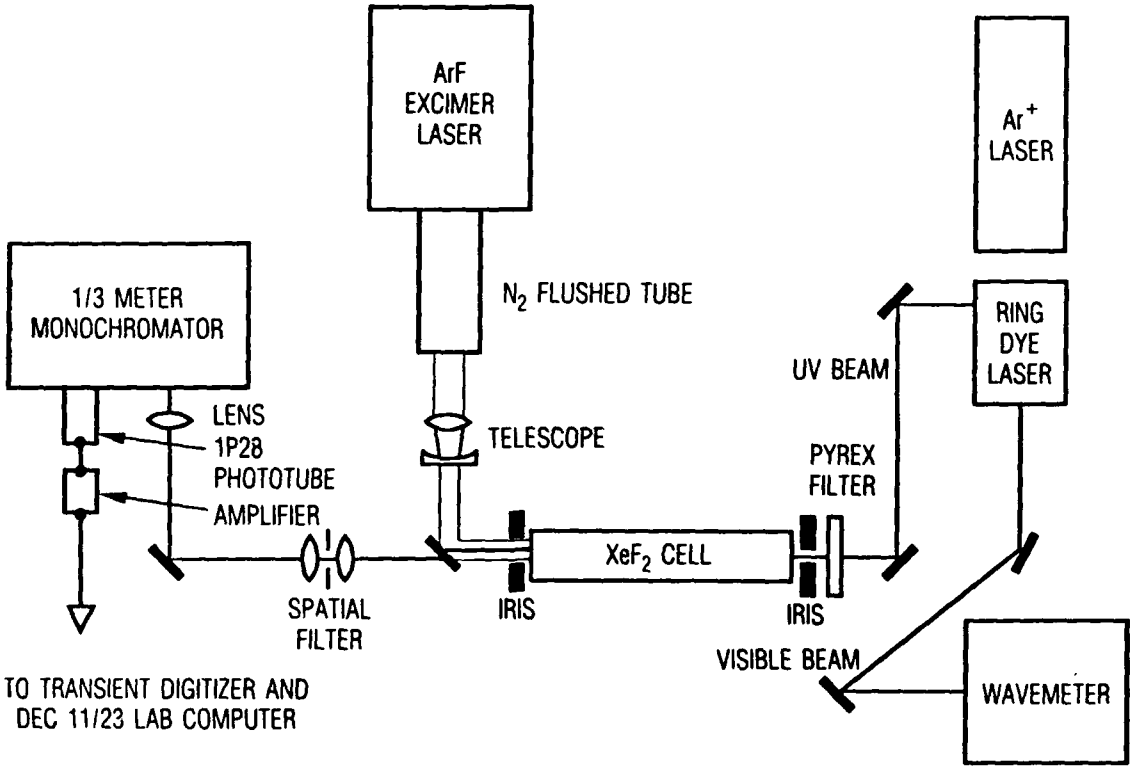

Fig. 1. Schematic of Experimental Apparatus

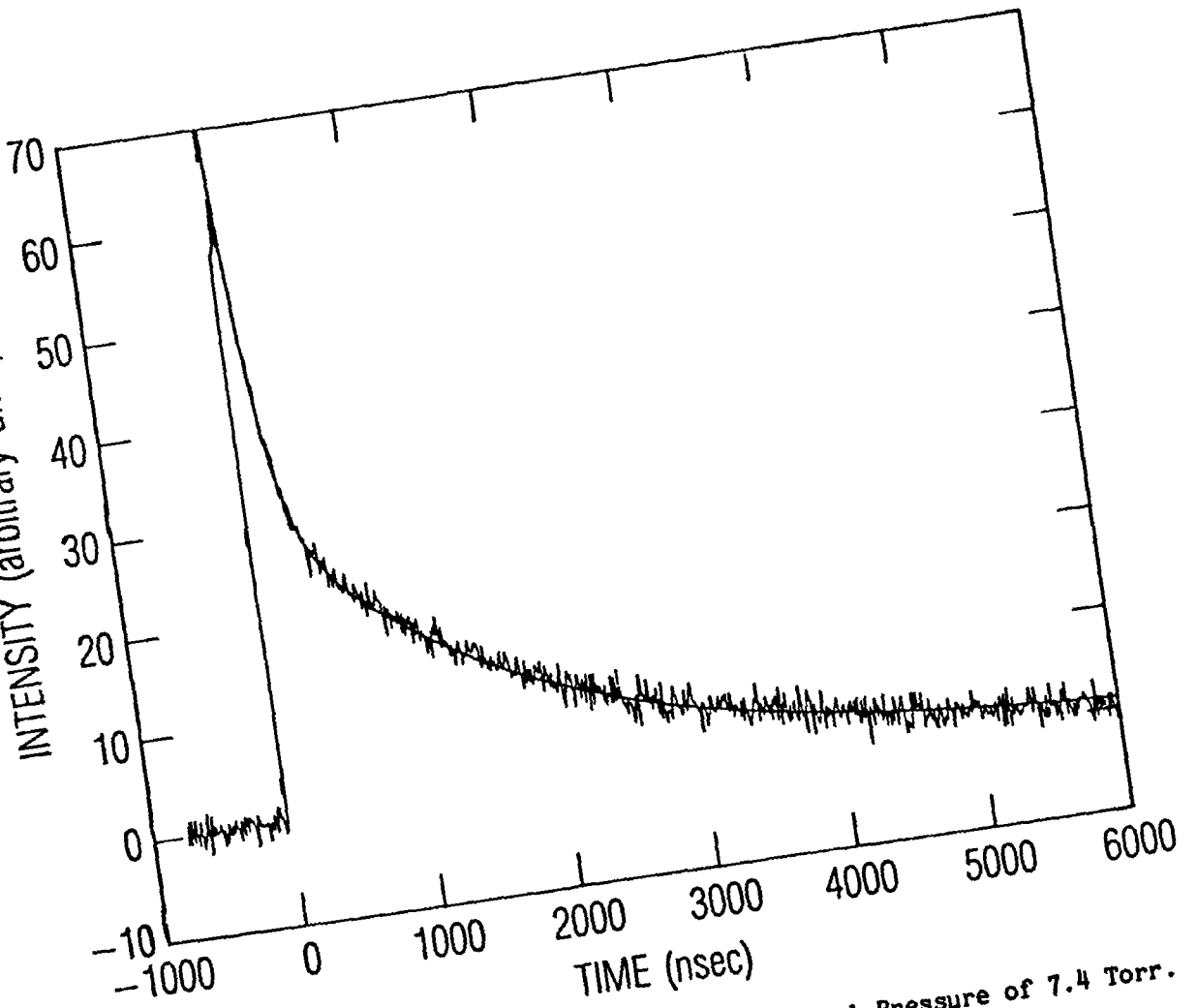

Fig. 2. Time History of XeF(X,v = 3) in N_2 at a Total Pressure of 7.4 Torr. Solid curve is a least squares fit to the profile.

(V-T) vibrational relaxation processes, decay with a single exponential rate.[5] Thus, the v = 3 level is initially overpopulated with respect to the slow decay portion of the traces at longer times, whereas the v = 0 and 1 levels are underpopulated. XeF laser transitions terminate on v = 2, 3, and 4 so that the removal rate of v = 3 is important to the operation of the excimer laser.

The initial decay rates of XeF(X,v = 3) measured in krypton and xenon are shown in Fig. 3; those measured at longer times are plotted in Fig. 4. Likewise, the initial and long-time decay rates of XeF(X,v = 3) measured in nitrogen and carbon dioxide are shown in Figs. 5 and 6, respectively. In the present experiments and those of Ref. 5, the peak signal was found to decrease as the diluent pressure was increased even though the partial pressure of the XeF_2 was kept constant. Therefore, the limiting pressure that could be studied was determined more by the loss of signal than by the time response limitations of the detection system. The signal loss was most pronounced for xenon, and only a few low-pressure decay rates could be measured. However, the decay rates obtained in xenon were consistent with the rates measured with krypton diluent.

Decay rates of XeF(X,v = 0) measured in SF_6 at long times are plotted in Fig. 7. For the v = 0 measurements, we chose an absorption feature in the 0 → 5 band near a nominal wavelength of 329.563 nm (vacuum), as indicated by the wavemeter. The XeF(X,v = 0) absorption profiles measured in SF_6 differed somewhat from the profiles recorded previously in the rare gases.[5] The rising portion of the profile (after the initial production of the v = 0 state) was more pronounced in the case of the rare gases so that an initial rise rate could be determined. However, the rising portion of the profile observed in the presence of SF_6 was too small to yield an exponential rise rate with any accuracy, so only the long-time decay rates were determined. A possible explanation is that SF_6 affects the initial distribution over the vibrational manifold of XeF.

Rate coefficients were determined from the slopes of the data plotted in Figs. 3 through 7 and are listed in Table I. The rate coefficients determined

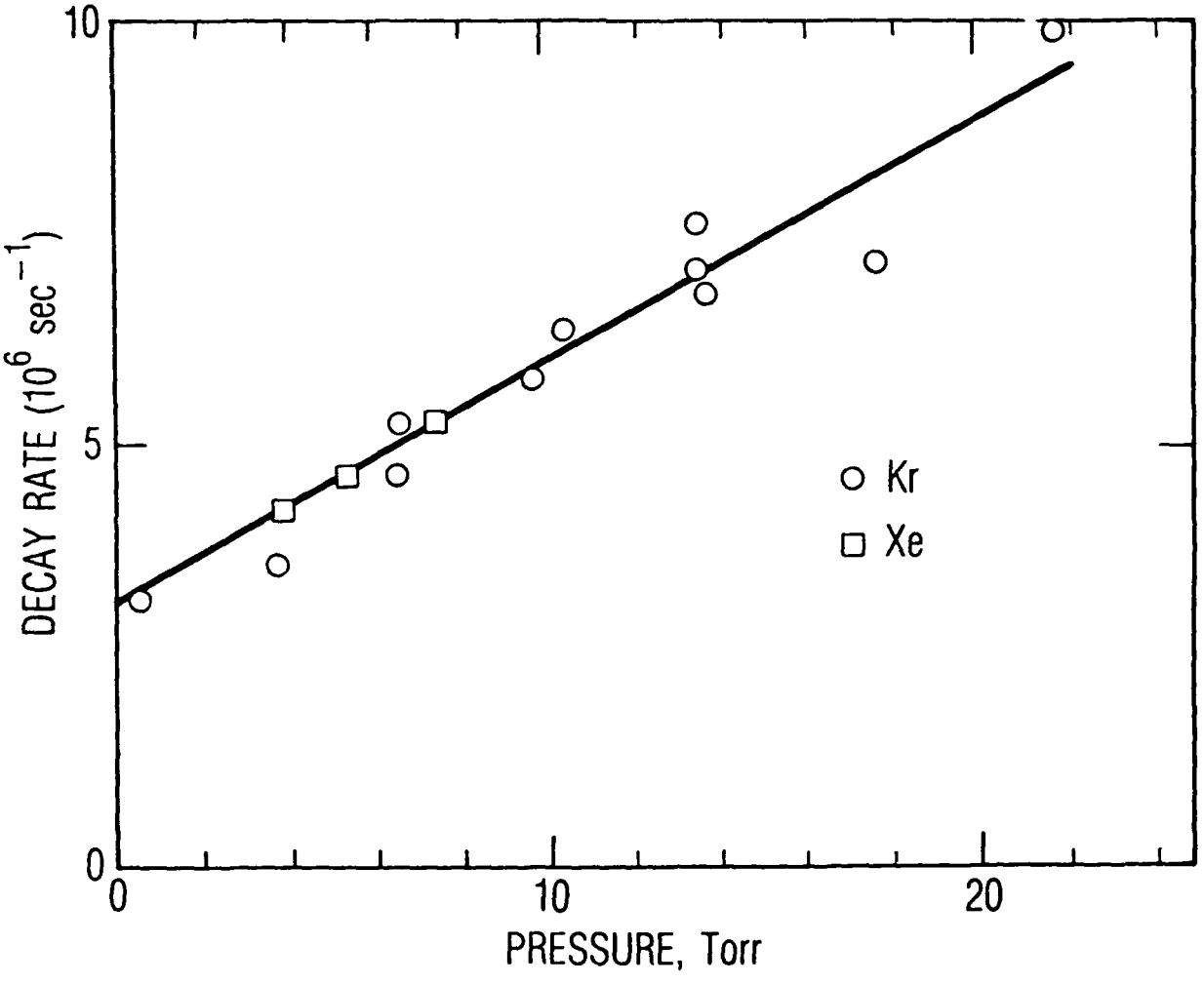

Fig. 3. Initial Decay Rates of XeF(X,v = 3) in Krypton and Xenon at 0.50 Torr Partial Pressure of XeF_2.

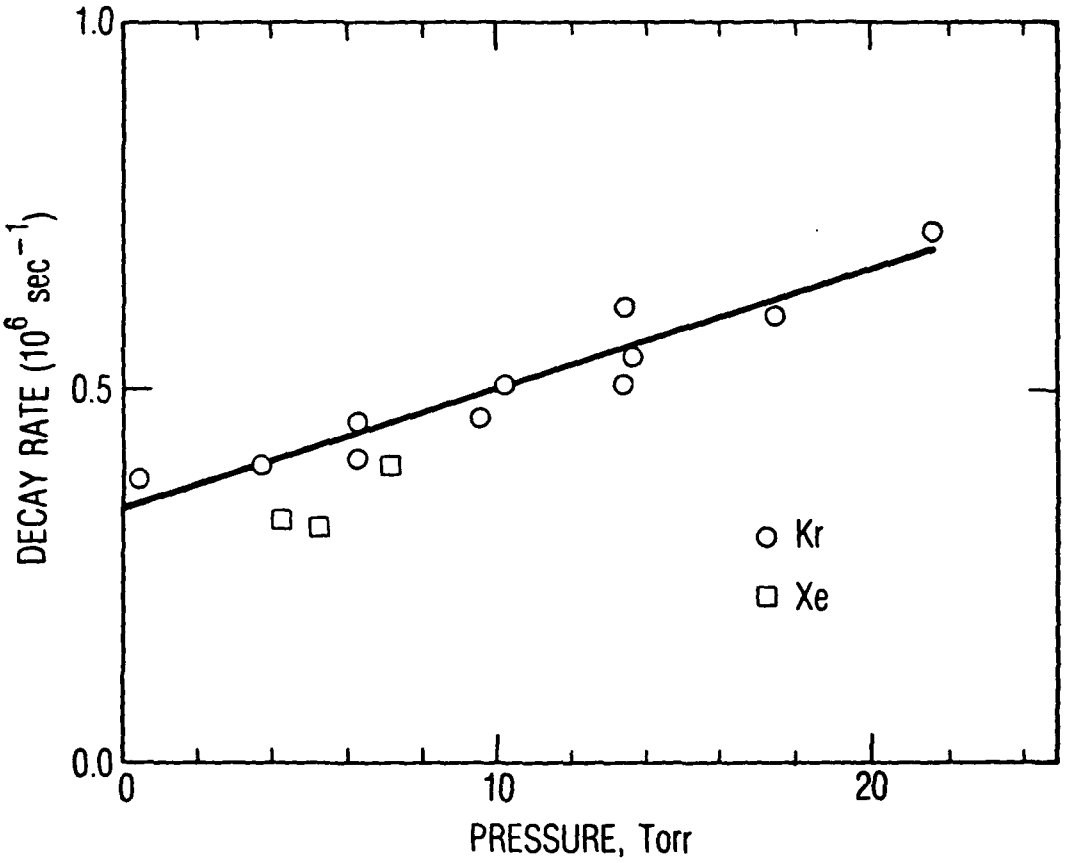

Fig. 4. Decay Rates of XeF(X,v = 3) at Long Times in Krypton and Xenon at 0.50 Torr Partial Pressure of XeF_2.

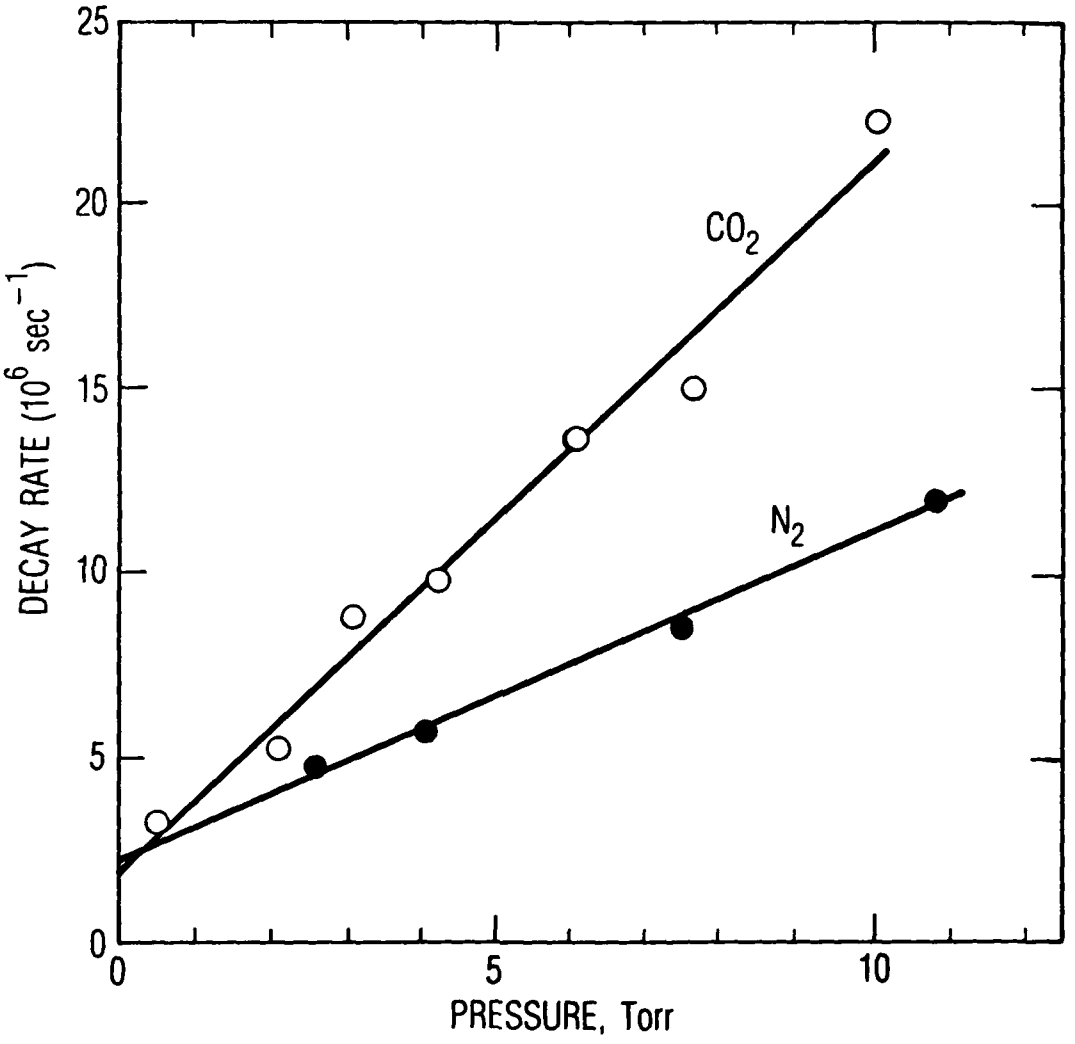

Fig. 5. Initial Decay Rates of XeF(X,v = 3) in Nitrogen and Carbon Dioxide at 0.50 Torr Partial Pressure of XeF_2.

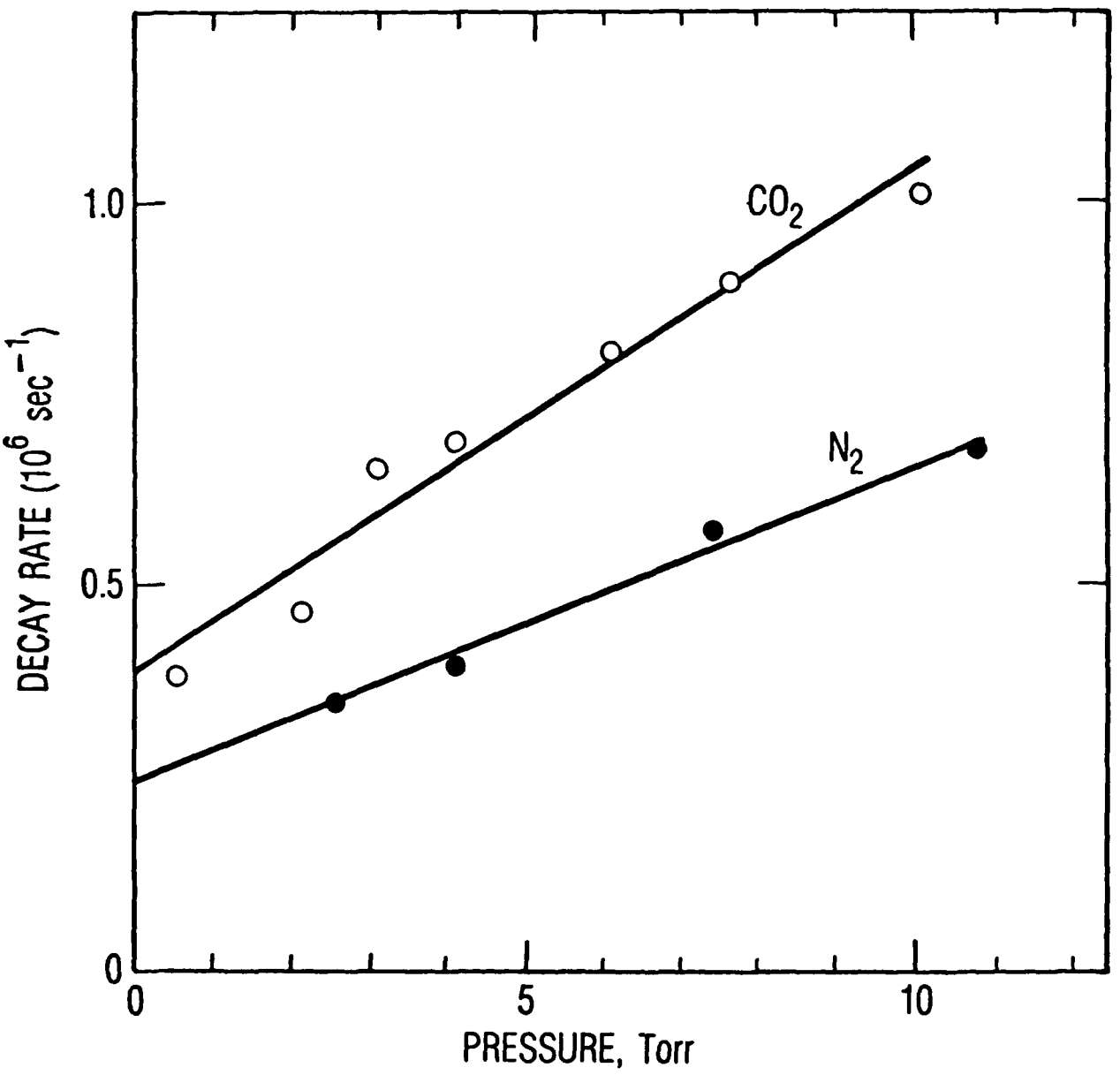

Fig. 6. Decay Rates of XeF(X,v = 3) at Long Times in Nitrogen and Carbon Dioxide at 0.50 Torr Partial Pressure of XeF_2.

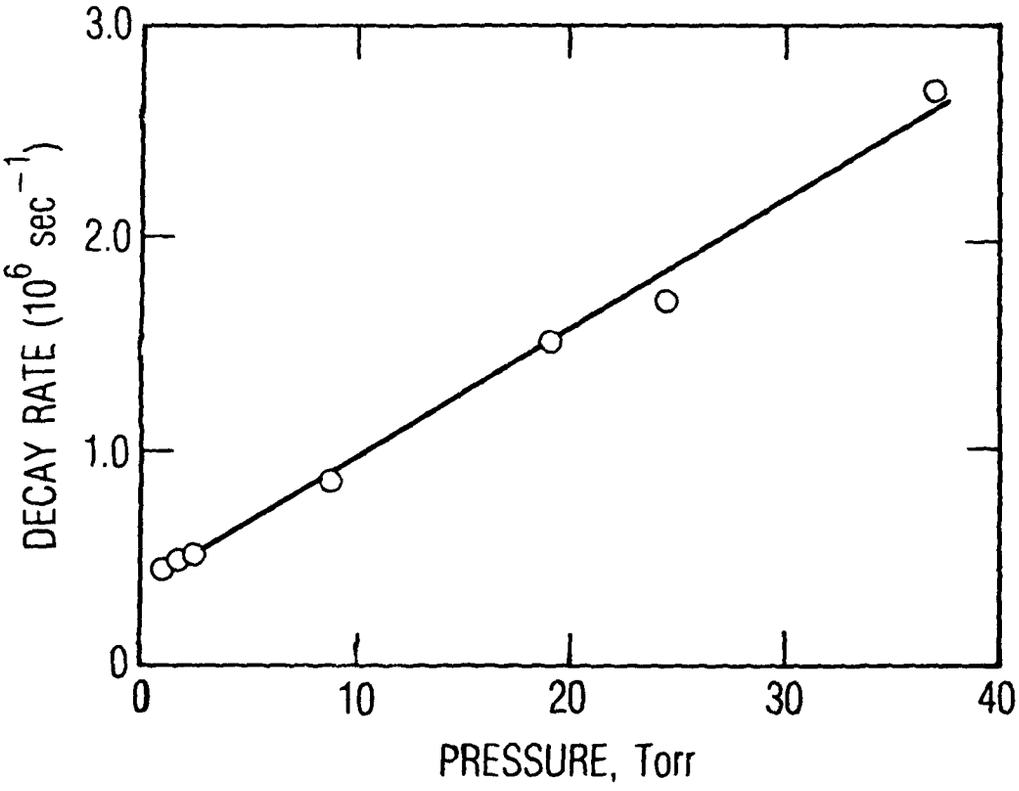

Fig. 7. Decay Rates of XeF(X,v = 0) at Long Times in Sulphur Hexafluoride at 0.50 Torr Partial Pressure of XeF_2

Table I. Rate coefficients for the various collision partners

Collision partner	v	Dissociation rate coefficient 10^4(sec-Torr)$^{-1}$	cm^3/molec.sec	Relaxation rate 10^5(sec-Torr)$^{-1}$	coefficient cm^3/molec.sec
He	0-4	2.0±0.2	6.2E-13	3.0±0.4	9.3E-12
Ne	0-4	2.0±0.2	6.2E-13	3.0±0.4	9.3E-12
Ar	0,1	2.5±0.2	7.7E-13		
Kr	3	1.6±0.2	4.9E-13	2.8±0.3	8.7E-12
Xe	3	1.6±0.3	4.9E-13	2.8±0.6	8.7E-12
N_2	3	4.1±0.5	1.3E-12	8.8±1.2	2.7E-11
SF_6	0	6.1±0.6	1.9E-12		
CO_2	3	6.8±1.0	2.1E-12	19±2	5.9E-11
XeF_2	0-4	50±7	1.5E-11	70±10	2.2E-10

from the initial decay rates of Figs. 3 and 5 are labeled relaxation rate coefficients in Table I; those determined from the decay rates at longer times--shown in Figs. 4, 6, and 7--are labeled dissociation rate coefficients. The intercepts of Figs. 3 and 5 and of Figs. 4, 6, and 7 represent vibrational relaxation and removal processes due to the presence of the nominal 0.5 Torr of XeF_2 in the gas mixtures. However, the more accurate rate coefficients reported in Ref. 5 for XeF_2 are preferred.

All of the measurements were performed at room temperature (23±2°C) with the partial pressure of XeF_2 maintained at 0.5±0.05 Torr. The gases used in the experiments included Spectra Gases, Inc., research grade krypton (99.995%) and xenon (99.995%); Air Products UHP nitrogen (99.995%); M. G. Gases CP grade sulfur hexafluoride (99.8%); and Alphagaz research grade carbon dioxide (99.998%).

III. DISCUSSION

The rate coefficients deduced from the present data are summarized in Table I, including the results from Ref. 5 for helium, neon, argon, and XeF_2. The vibrational relaxation rates are listed as reciprocal relaxation times and also as rate coefficients in units of cm^3/molecule-sec, obtained by multiplying the reciprocal relaxation time by RT, the product of the gas constant and the temperature. We have neglected the factor of $(1 - \exp(-h\nu/RT))$, which would be required for a state-to-state rate coefficient for a harmonic oscillator. Although the removal rates were obtained from the decays of vibrational levels v = 0 and 3, they are representative of the removal rates of the whole electronic ground state of XeF. The fast vibrational relaxation of XeF(X,v) by the diluent gas drives the initial populations into a coupled distribution over the vibrational manifold. Thereafter, the populations of the several vibrational levels decay with a common exponential decay rate coefficient. Although the vibrational populations decay at the same exponential rate, they may not fit a Boltzmann distribution over the vibrational manifold. This may be particularly true for the higher vibrational levels, which can be expected to have much larger state-to-state rate coefficients than the lower levels. The present measurements, however, were not designed to determine the relative distribution over the vibrational manifold.

All the removal rate coefficients obtained for the rare gases have similar values. The removal rate coefficient for argon is larger than those for helium and neon by only 25%; those for krypton and xenon are smaller by 20%. Although the removal rate coefficients are very similar, the cross sections calculated from these rate coefficients differ by as much as a factor of 3.5 for helium and argon because of their different collision frequencies. The calculated dissociation probabilities are listed in Table II and range from 1.3×10^{-3} for helium to 3.6×10^{-3} for argon. The mass and velocity of the collision partner are expected to affect the dissociation probability in a collision with XeF, so that the similarity of the rate coefficients (collision

Table II. Collision probabilities for XeF dissociation

Collision Partner	Collision diameter[b]	Molec. Wt.	Reduced mass	k_{dis}	k_{kin} $(sec\text{-}Torr)^{-1}$	Prob.[a]
He	2.576	4	3.90	2.0E+04	1.5E+07	1.3E-03
Ne	2.789	20.2	17.81	2.0E+04	7.6E+06	2.6E-03
Ar	3.418	40	31.59	2.5E+04	6.8E+06	3.6E-03
Kr	3.61	83.8	53.80	1.6E+04	5.4E+06	3.0E-03
Xe	4.055	131.3	70.08	1.6E+04	5.3E+06	3.0E-03
XeF	4.3	150.3	75.15			
N_2	3.681	28.0	23.62	4.1E+04	8.4E+06	4.9E-03
SF_6	5.13	146.1	74.09	6.1E+04	6.6E+06	9.2E-03
CO_2	3.952	44.0	34.04	6.8E+04	7.5E+06	9.1E-03
XeF_2	4.3	169.3	79.62	5.0E+05	5.3E+06	9.4E-02

[a] Prob. = k_{dis}/k_{kin}, where $k_{kin} = 2.57 \times 10^6 \bar{D}^2/m^{1/2}$ $(sec\text{-}Torr)^{-1}$, $\bar{D} = (D_1 + D_2)/2$, and m is the translational reduced mass in amu.

[b] Collision diameters taken from Ref. 7, except for XeF and XeF_2, which have been estimated.

rate × probability) must be coincidental. Similarly, there is not much variation in the rate coefficients for vibrational relaxation by the rare gases, which are also listed in Table I. The dissociation rate coefficients for the molecular collision partners are larger than those for the rare gases by factors between 2 and 3.5 for N_2, SF_6, and CO_2 and by a factor of about 25 for XeF_2.

The rate coefficient for the recombination of Xe and F atoms can be calculated from the XeF dissociation rate coefficient and the equilibrium constant. The equilibrium constant was calculated from spectroscopic and thermochemical data for the atoms[8] and for XeF[9] using statistical thermodynamics. For temperatures between 273 and 500 K, the equilibrium constant can be expressed as

$$K_{eq} = 1.197 \times 10^{-23} \times T^{0.267} \exp(1464/T) \text{ cm}^3 \qquad (1)$$

(The $T^{0.267}$ term was inadvertently omitted from this expression when it was previously printed in Ref. 5; however, the correct equation was used in the calculations reported in that reference.) With a value of 7.45×10^{-21} cm^3 for K_{eq} at 298 K, we calculate a value of 4.6×10^{-33} $(cm^3/molecule)^2/s$ or $10^{9.2}$ $(L/mol)^2/s$ for the recombination rate coefficient for Xe + F in the presence of helium or neon. Benson[10] has tabulated atom recombination rate coefficients and noted that they all seem to lie near $10^{9.5\pm0.5}$ $(L/mol)^2/s$ at 300 K. With the exception of M = XeF_2, the present recombination rate coefficients range between $10^{9.12}$ $(L/mol)^2/s$ for Kr and Xe and $10^{9.75}$ $(L/mol)^2/s$ for CO_2--values which are well within the limits noted by Benson.

Dissociation rate coefficients typically can be described[11] by an equation of the form $A \times T^{0.5-n} \times \exp(-E/RT)$, where E is the bond dissociation energy and n depends on the degrees of freedom participating in the activation of the molecule (1 for each vibration and 1/2 for each rotation). Rate coefficients are reported in Ref. 5 for the dissociation of XeF(X) by helium and neon between 296 and 368 K. A least squares fit to these data gives E = 962 cm^{-1} for T^0 or E = 1077 cm^{-1} for $T^{-0.5}$. Since the spectroscopic value[9] of the dissociation energy is 1063 cm^{-1}, the $T^{-0.5}$ temperature dependence appears

reasonable for a unimolecular reaction in the low-pressure regime with one vibrational degree of freedom contributing to the activation.

Fulghum et al.[3] suggested that the vibrational relaxation rate coefficients such as those listed in Table I should not be interpreted as state-to-state rate coefficients but rather as weighted averages of the VT rate coefficients for several vibrational levels. This is consistent with the observation[5] that the relaxation rates for XeF(X,v) relaxing in helium and neon for v = 3 and 4 agree with those for v = 0. It is clear from Table I that there is a qualitative relation between the dissociation rate coefficients and the vibrational relaxation rate coefficients obtained for the different collision partners. The vibrational relaxation rate coefficients are about 16 to 20 times larger than the dissociation rate coefficients--except for CO_2, which has a ratio of 28. The vibrational relaxation rate coefficient for XeF_2 has a value of 70×10^5 $(sec\text{-}Torr)^{-1}$, which is 30% larger than the gas kinetic rate coefficient calculated on the basis of a 4.3 Å collision diameter. Fulghum et al.[4] suggested that this large value is the result of the near resonance between the bending mode of XeF_2 (212 cm^{-1}) and the 0->1 vibrational transition of XeF (204±4 cm^{-1}). It is not clear whether this near resonance can account for the rapid dissociation as well as vibrational relaxation.

Although the rate coefficients presented here cannot be interpreted as state-to-state rate coefficients, they can be used to test any theoretical or model calculations. Fulghum et al.[4] used an information theoretic approach to generate a set of state-to-state rate coefficients for the relaxation of XeF(X,v) by helium and neon. Their rate coefficient expression can fit the present data if a larger value for their C_V is used to generate the VT relaxation rate coefficients. Their value of 1×10^{-12} cm^3/molecule-sec for C_V has to be increased to 7.5×10^{-12} cm^3 molecule-sec to fit our data. Wilkins[12] has recently calculated vibrational relaxation and dissociation rates using classical trajectories and obtained 7.4×10^{-12} cm^3/molecule-sec for v = 1 to 0 relaxation by neon and 1.0×10^{-11} by helium. These state-to-state rate coefficients are in reasonable agreement with the present vibrational relaxation data.

Millikan and White[13] were able to correlate the vibrational relaxation of a large number of diatomic molecules (none contained a hydrogen atom). Their correlation predicts VT rates for XeF at 300 K that depend on the reduced mass of the collision pair. Their correlation yields values of 2.2×10^{-12} cm^3/molecule-sec for helium and 0.53×10^{-12} cm^3/molecule-sec for xenon, with the rates for the other rare gases falling between these values. These rates are too slow compared to our measured values of about 9×10^{-12} cm^3/molecule-sec. Furthermore, our rate coefficients do not show much dependence on reduced mass of the collision pair.

State-to-state dissociation rate coefficients were also calculated by Wilkins.[12] He concluded that dissociation could occur from any vibrational level, although it was much more probable for a collision in which the XeF is in a high vibrational level. Fulghum[4] fitted his data with a state-to-state collision-induced dissociation model based on a model described by Kiefer et al.[14] that includes a vibrational bias parameter. The relative dependence of the rate coefficients on vibrational level predicted by this model is in reasonable agreement with the dependence calculated by Wilkins, although the rate coefficients are larger than those of Wilkins by about a factor of 1.4. The present data can be fitted with Fulghum's dissociation rate model if the above-mentioned faster VT rate coefficients are used. (The overall removal rate depends in part on the vibrational relaxation rate coefficients.) An alternative dissociation model is the "ladder model," in which vibrational relaxation processes pump population from the lower vibrational levels into the upper levels with dissociation occurring only from the highest vibrational relaxation levels. The present measurements of the overall dissociation rate are not sufficient to choose between such alternative dissociation models.

Brashears and Setser[15] have measured the quenching rates of XeF(B) for a number of collision partners. They found the quenching rate coefficients for the rare gases to increase in the order of neon, helium, argon, krypton, and xenon, with a total variation of a factor of 60. Their smallest quenching rate coefficient, 1×10^{-12} cm^3/molecule-sec for neon, is only slightly larger than our value of 6.2×10^{-13} cm^3/molecule-sec for the dissociation rate coefficient of XeF(X) in neon; however, the xenon quenching rate for the B

state is much larger (on the order of a factor of 100 larger) than the dissociation rate coefficient for XeF(X) in xenon. As mentioned previously, the peak absorption signal was found to decrease as the diluent pressure increased, even though the XeF_2 partial pressure was kept constant. The signal loss was most pronounced for xenon, with neon and helium having the least effect. In fact, the effect was observed to increase in the same order as the quenching rate coefficients measured by Brashears and Setser.[15] However, it is not clear that the quenching rate coefficients are fast enough to compete at these low pressures with the radiative decay rate of the B state, which has a 14 nsec lifetime.

In summary, the rate coefficients for the dissociation of XeF(X) have been measured for several collision partners. There appears to be no advantage in adding rare gases other than neon and the required xenon to the laser mixture to increase the removal rate of the ground state of XeF. The dissociation rate coefficient for XeF in XeF_2 is considerably larger than in the rare gases, but XeF_2 addition would be impractical because of its low vapor pressure and its spectral absorption at the laser wavelengths. The dissociation rate coefficients appear reasonable for a unimolecular reaction in the low-pressure regime.

REFERENCES

1. J. A. Blauer, T. T. Yang, C. E. Turner, and D. A. Copeland, Appl. Opt. 23, 4352 (1984).
2. J. C. Hsia, J. A. Mangano, J. H. Jacob, and M. Rokni, Appl. Phys. Lett. 34, 208 (1979).
3. S. F. Fulghum, M. S. Feld, and A. Javan, Appl. Phys. Lett. 35, 247 (1979).
4. S. F. Fulghum, M. S. Feld, and A. Javan, IEEE J. Quantum Electron. 16, 815 (1980).
5. J. F. Bott, R. F. Heidner, J. S. Holloway, J. B. Koffend, and M. A. Kwok, J. Chem. Phys. 89, 4154 (1988).
6. J. G. Eden and R. W. Waynant, Opt. Lett. 2, 13 (1978).
7. J.O. Hirschfelder, C.F. Curtis, and R.F. Bird, Molecular Theory of Gases, 2nd ed., John Wiley and Sons, New York (1964), p. 1212.
8. C. E. Moore, Atomic Energy Levels, National Bureau of Standards Circular No. 467, U.S. GPO, Washington, DC, Vol. I (1949); Vol. III (1958).
9. P. Tellinghuisen and J. Tellinghuisen, Appl. Phys. Lett. 43, 898 (1983).
10. S. W. Benson, Thermochemical Kinetics, John Wiley & Sons, New York (1976), p. 180.
11. I. Amdur and G. G. Hammes, Chemical Kinetics, Principles and Selected Topics, McGraw-Hill Book Company, New York (1966), pp. 39 and 202.
12. R. L. Wilkins, J. Chem. Phys. 89, 6267 (1988).
13. R. C. Millikan and D. R. White, J. Chem. Phys. 39, 3209 (1963).
14. J. H. Kiever, H. P. G. Joosten, and W. D. Breshears, Chem. Phys. Lett. 30, 424 (1975).
15. H. C. Brashears and D. W. Setser, J. Chem. Phys. 76, 4932 (1982).

LABORATORY OPERATIONS

The Aerospace Corporation functions as an "architect-engineer" for national security projects, specializing in advanced military space systems. Providing research support, the corporation's Laboratory Operations conducts experimental and theoretical investigations that focus on the application of scientific and technical advances to such systems. Vital to the success of these investigations is the technical staff's wide-ranging expertise and its ability to stay current with new developments. This expertise is enhanced by a research program aimed at dealing with the many problems associated with rapidly evolving space systems. Contributing their capabilities to the research effort are these individual laboratories:

Aerophysics Laboratory: Launch vehicle and reentry fluid mechanics, heat transfer and flight dynamics; chemical and electric propulsion, propellant chemistry, chemical dynamics, environmental chemistry, trace detection; spacecraft structural mechanics, contamination, thermal and structural control; high temperature thermomechanics, gas kinetics and radiation; cw and pulsed chemical and excimer laser development including chemical kinetics, spectroscopy, optical resonators, beam control, atmospheric propagation, laser effects and countermeasures.

Chemistry and Physics Laboratory: Atmospheric chemical reactions, atmospheric optics, light scattering, state-specific chemical reactions and radiative signatures of missile plumes, sensor out-of-field-of-view rejection, applied laser spectroscopy, laser chemistry, laser optoelectronics, solar cell physics, battery electrochemistry, space vacuum and radiation effects on materials, lubrication and surface phenomena, thermionic emission, photosensitive materials and detectors, atomic frequency standards, and environmental chemistry.

Computer Science Laboratory: Program verification, program translation, performance-sensitive system design, distributed architectures for spaceborne computers, fault-tolerant computer systems, artificial intelligence, microelectronics applications, communication protocols, and computer security.

Electronics Research Laboratory: Microelectronics, solid-state device physics, compound semiconductors, radiation hardening; electro-optics, quantum electronics, solid-state lasers, optical propagation and communications; microwave semiconductor devices, microwave/millimeter wave measurements, diagnostics and radiometry, microwave/millimeter wave thermionic devices; atomic time and frequency standards; antennas, rf systems, electromagnetic propagation phenomena, space communication systems.

Materials Sciences Laboratory: Development of new materials: metals, alloys, ceramics, polymers and their composites, and new forms of carbon; nondestructive evaluation, component failure analysis and reliability; fracture mechanics and stress corrosion; analysis and evaluation of materials at cryogenic and elevated temperatures as well as in space and enemy-induced environments.

Space Sciences Laboratory: Magnetospheric, auroral and cosmic ray physics, wave-particle interactions, magnetospheric plasma waves; atmospheric and ionospheric physics, density and composition of the upper atmosphere, remote sensing using atmospheric radiation; solar physics, infrared astronomy, infrared signature analysis; effects of solar activity, magnetic storms and nuclear explosions on the earth's atmosphere, ionosphere and magnetosphere; effects of electromagnetic and particulate radiations on space systems; space instrumentation.